Current Biology, Vol. 15, 833–838, May 10, 2005, ©2005 Elsevier Ltd All rights reserved. DOI 10.1016/j.cub.2005.03.039

The Heparan Sulfate Proteoglycans Dally-like and Syndecan Have Distinct Functions in Axon Guidance and Visual-System Assembly in *Drosophila*

Joel M. Rawson,[1,3] Brian Dimitroff,[1] Karl G. Johnson,[2] Jaime M. Rawson,[1] Xuecai Ge,[2] David Van Vactor,[2] and Scott B. Selleck[1,*]

[1]Department of Pediatrics and
Department of Genetics, Cell Biology
and Development
Developmental Biology Center
University of Minnesota
321 Church St. SE
Minneapolis, Minnesota 55455

[2]Department of Cellular Biology and
Program in Neuroscience
Harvard Medical School
240 Longwood Avenue
Boston, Massachusetts 02115

[3]Graduate Interdisciplinary Program in Neuroscience
University of Arizona
Life Sciences North 351
Tucson, Arizona 85724

Summary

Heparan sulfate proteoglycans (HSPGs), a class of glycosaminoglycan-modified proteins, control diverse patterning events via their regulation of growth-factor signaling and morphogen distribution [1]. In *C. elegans*, zebrafish, and the mouse, heparan sulfate (HS) biosynthesis is required for normal axon guidance [2–4], and mutations affecting Syndecan (Sdc), a transmembrane HSPG, disrupt axon guidance in *Drosophila* embryos [5, 6]. Glypicans, a family of glycosylphosphatidylinositol (GPI)-linked HSPGs, are expressed on axons and growth cones in vertebrates, but their role in axon guidance has not been determined [7, 8]. We demonstrate here that the *Drosophila* glypican Dally-like protein (Dlp) is required for proper axon guidance and visual-system function. Mosaic studies revealed that Dlp is necessary in both the retina and the brain for different aspects of visual-system assembly. Sdc mutants also showed axon guidance and visual-system defects, some that overlap with *dlp* and others that are unique. *dlp*$^{+}$ transgenes were able to rescue some *sdc* visual-system phenotypes, but *sdc*$^{+}$ transgenes were ineffective in rescuing *dlp* abnormalities. Together, these findings suggest that in some contexts HS chains provide the biologically critical component, whereas in others the structure of the protein core is also essential.

Results and Discussion

We examined the distribution of Dlp in the developing visual system by using a monoclonal antibody [9] that specifically recognizes Dlp in tissues [10]. In *Drosophila*, the adult eye is comprised of approximately 800 sensory units, or ommatidia, each with eight distinct photoreceptors, R1–R8. In the eye imaginal disc, Dlp was found on photoreceptor cell bodies and on cells within the morphogenetic furrow (Figures 1A and 1B). Axons from R1–R6 terminate in the lamina, the first optic ganglion (Figure 2A, arrow), whereas those from R7 and R8 project to the medulla (Figure 2A, arrowhead). In the optic lobe, Dlp was present on photoreceptor axons at the boundary between the lamina and adjacent tissues (Figures 1C, 1E, and 1E′, arrows) and along the lamina plexus (Figures 1D and 1D′, asterisk). Dlp was also observed in the medulla neuropil (Figure 1E, arrowhead), medulla glia, medulla neuropil glia (Figures 1F, 1F′, G, and G′, arrowheads), neuroblasts of the proliferative centers (Figure 1H), and in the mushroom body neuropil (Figures 1H and 1I).

To evaluate the function of Dlp in axon guidance, we used a photoreceptor-specific monoclonal antibody (24B10) [11] to visualize photoreceptor projections in *dlp* mutants. In 50% of *dlp* mutant hemispheres, the lamina plexus was irregular and thickened (Figure 2B, arrow). Additionally, 80% of *dlp* mutant larvae had fibers that aberrantly crossed between ommatidial bundles (Figure 2B, inset) and/or photoreceptor process expansions outside the normal termination zone of the lamina plexus (for phenotypic quantification, see Figure S1A in the Supplemental Data available with this article online). Examination of *dlp* mutant pupae revealed that 80% of optic lobes contain irregularities in the R7 and R8 medulla termini (Figures 2D and 2E). We also observed crossover of R7 axons to neighboring medulla cartridges (~50%) and misrouting of R7/R8 axons (~20%) (quantified in Figure S1B).

We assessed visual-system function in *dlp* mutants by recording electroretinogram (ERG) profiles in adult flies. A wild-type ERG is composed of the photoreceptor response generated by a light-induced depolarization of the photoreceptor neurons and of the two transient voltage changes, the "on-transient" and the "off-transient" (Figure 2J), resulting from currents related to synaptic transmission during the initiation and termination of the light stimulus [12]. *dlp* mutants showed statistically significant defects in the photoreceptor response and in both on- and off-transients (Figure 2J,K), suggesting that Dlp is required for proper photoreceptor currents and synaptic transmission.

Axon guidance in the visual system depends on photoreceptor specification, as well as on glial-cell migration [13] and lamina-neuron differentiation [14]. Although *dlp* mutants have reduced and roughened eyes, thin sections of *dlp* eyes demonstrated that all photoreceptors are present and retain proper polarity in each ommatidium (see Figure S2). Staining with several photoreceptor-specific markers confirmed that *dlp* mutant photoreceptors differentiate properly (Figure S3). Likewise, glial cells and lamina neurons were found in the correct number and location in *dlp* mutants (Figure S4), indicating that patterning defects of these critical cells cannot account for the observed axon-guidance defects.

Because Dlp is expressed in several visual-system

*Correspondence: selle011@umn.edu

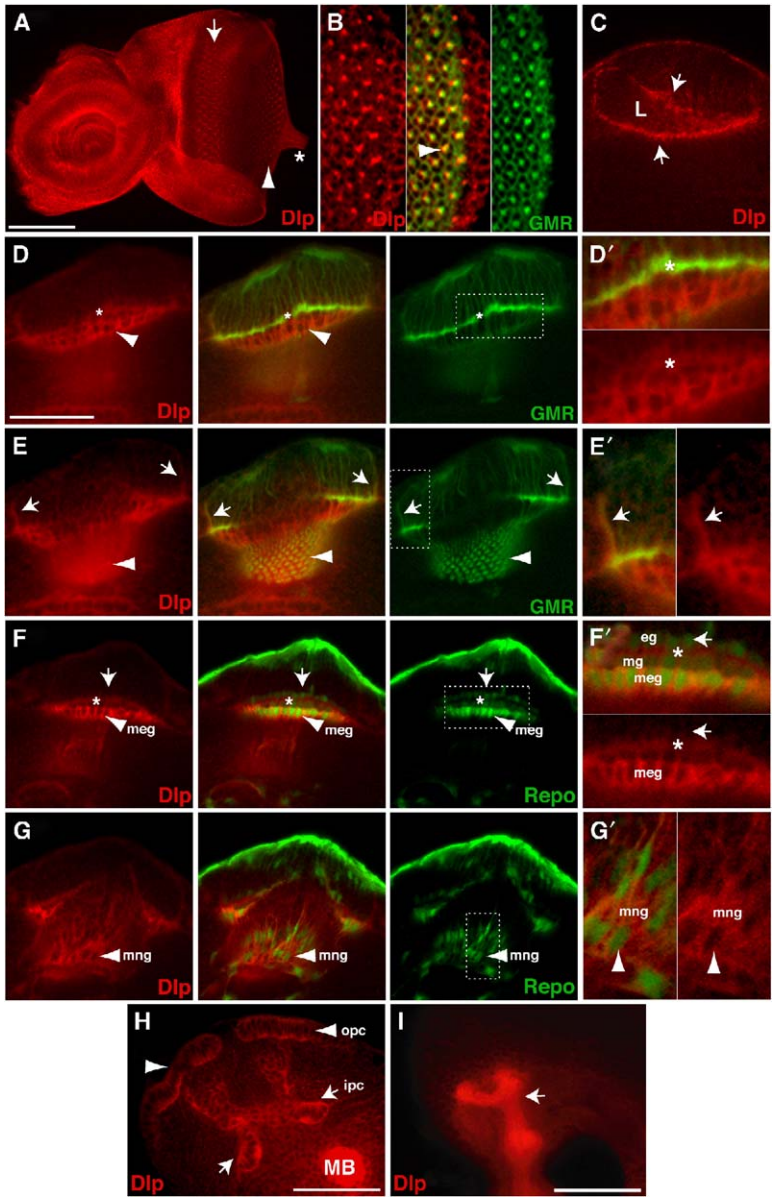

Figure 1. Expression of Dlp in the Developing Adult Visual System

All images are single optical sections of wild-type tissues stained with anti-Dlp antibody (red) and green fluorescent protein (GFP) expressed under control of either GMR-GAL4 (photoreceptors) or Repo-GAL4 (glia). (D′–G′) show enlarged views of outlined regions.

(A) In the eye-antennal disk, Dlp is expressed in the morphogenetic furrow (arrow), on differentiated photoreceptor cell bodies (arrowhead), and on photoreceptor axons exiting at the optic stalk (asterisk).

(B) Higher-magnification view of posterior portion of eye-antennal disc. Note the colocalization of Dlp with photoreceptor-specific GFP (arrowhead).

(C) Lateral view of third-instar larval brain, anterior to left. Dlp is primarily found on photoreceptor axons along the boundary (arrows) of the lamina (L).

(D–G) Dorsal-posterior view of third-instar larval brains; lateral surface of optic lobe is up. (D, D′) Dlp is observed on R1–R6 termini at the lamina plexus (asterisks) and just below the lamina plexus in the medulla glia (arrowheads) (see [F] below). (E, E′) Dlp is greatest on photoreceptors along the boundary of the lamina (arrows, deeper focal plane than in [D, D′]). Dlp colocalizes with R7/R8 termini in the medulla (arrowheads) and is also present broadly in this region (see [G] below). (F, F′) Dlp is expressed in the medulla glia (meg, arrowheads) but not in the epithelial glia (eg) or marginal glia (mg) (arrows), as evidenced by colocalization with glia-specific GFP. Dlp is also on the lamina plexus (asterisk). (G, G′) Dlp is found on the medulla neuropil glia (mng) (arrowheads) in the region of R7/R8 termination.

(H) Dlp is present on neuroblasts of the inner and outer proliferative centers (ipc, arrows; opc, arrowheads) and is highly expressed in the mushroom body neuropil (MB in [H], arrow in [I]). Scale bars represent 50 microns.

elements and cell types, we conducted somatic mosaic studies to determine which cells require *dlp* for visual-system assembly. Using a method that generates clones encompassing a majority of cells in the retina [15], we observed crossover of axons between ommatidial bundles (Figure 2C, arrowheads) and photoreceptor process expansions outside the lamina plexus (Figure 2C, arrows) in 67% of animals with *dlp* mutant photoreceptors projecting to a heterozygous brain (n = 33) (as opposed to 8% in wild-type "control" clones, n = 37). Conversely, R7/R8 termination defects were absent from the medulla of 40 hr pupae with *dlp* mutant retinas and *dlp*/+ optic lobes (Figure 2F). These results indicate that Dlp is required in the eye to specify proper axon guidance to the lamina, but not to the medulla.

The photoreceptor-specific requirement for Dlp was further evaluated via the mosaic analysis with a repressible cell marker (MARCM) technique to visualize axons from small *dlp* mutant clones [16]. *dlp* mutant photoreceptors displayed ectopic axon outgrowths directed away from their proper targets in the lamina (Figures 2G, 2H, and 2I, arrowheads) (37% of *dlp*/*dlp* axons, n = 206; 11% of controls, n = 362). Ectopic axon processes were four times more prevalent on axon bundles near the boundaries of the lamina than on those in more-central regions. This suggests that expression of Dlp on photoreceptors may be important for the detection of repellant cues that prevent aberrant axon outgrowth.

Finally, we evaluated the tissue-specific requirement for Dlp in physiological function of the visual system. Using a mosaic strategy that generated eyes composed solely of *dlp* mutant photoreceptors [17], we did not see statistically significant defects in ERG record-

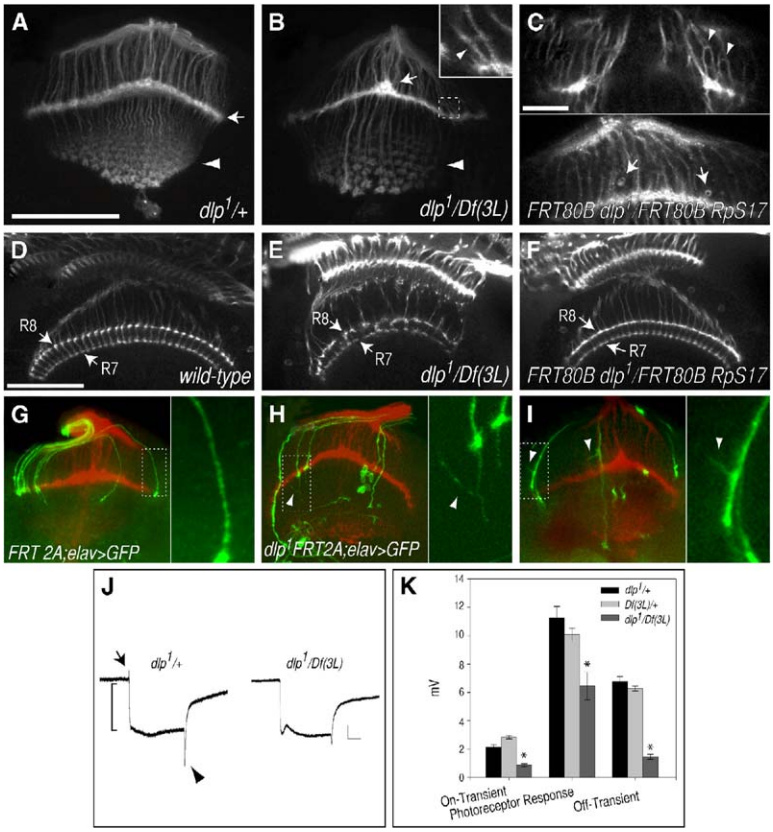

Figure 2. Analysis of *dlp* in Visual-System Assembly and Function

(A–B) Merged optical sections of photoreceptor-specific antibody staining (24B10) in third-instar optic lobes, dorsal/posterior view. (A) A *dlp* heterozygote showing wild-type patterning of termini forming the lamina plexus (arrow) and medulla projections (arrowhead) is shown. (B) A *dlp* mutant with thickening of the lamina plexus (arrow) and crossovers between ommatidial axon bundles (inset) is shown. R7/R8 termini in the medulla are relatively unaffected (arrowhead).

(C) Single optical sections from animals where most photoreceptors are *dlp* mutant but brains are *dlp*/+. Photoreceptor fibers cross between ommatidial axon bundles (arrowheads) and show process expansions outside the lamina plexus (arrows).

(D–F) Single optical sections, 24B10 staining of 40 hr pupal brains, dorsal view. (D) A wild-type optic lobe is shown. Note the two distinct layers of R7 and R8 termini (labels) in the medulla. (E) *dlp* mutant pupae have defects in R7/R8 termini. (F) Homozygous *dlp* mutant photoreceptors projecting to a heterozygous brain show normal R7/R8 termini.

(G–I) Merged optical sections showing individual *dlp*/*dlp* or control (*FRT2A*) photoreceptor clones expressing GFP (red is 24B10). Smaller panels (right) show enlarged views of outlined regions. (G) Control photoreceptor-axon bundles take smooth, straight paths to their targets in the optic lobe. (H) Some *dlp* mutant photoreceptor axons deviate from their proper path (arrowhead) and fail to reach the correct target. (I) Ectopic axon outgrowths (arrowheads) commonly project from *dlp*/*dlp* photoreceptors.

(J) ERG traces from a heterozygous control and a *dlp* mutant. Note the absence of the "on-transient" (arrow) and the "off-transient" (arrowhead) in the *dlp* mutant. The bracket shows photoreceptor response. Scale = 3 mV, 200 ms.

(K) Voltage measurements of ERG components in *dlp* heterozygote controls and *dlp* homozygous-mutant animals. The asterisk denotes statistically significant difference ($p < 0.05$, Student's t test). Scale bars represent 50 microns in (A) and (D) and 20 microns in (C).

ings compared to controls (n = 16, data not shown). These results demonstrate that the ERG defects of *dlp* mutants are produced by loss-of-function in the optic lobe, not in the eye.

Drosophila Syndecan (Sdc) represents another class of HSPG, and it is required for normal axon guidance in the embryo [5, 6]. Antibody specific for Sdc [5] revealed that this proteoglycan is present on photoreceptors in the retina (Figures 3A and 3B) and on photoreceptor projections to the optic lobe. Like Dlp, Sdc is enriched throughout the lamina plexus (Figures 3C and C′) and at the boundary between the lamina and adjacent tissues (Figures 3D and D′, arrowheads). Sdc immunoreactivity was also detectable at a low level on cells just medial to the lamina plexus, the medulla glia (Figure 3D, asterisk), but was absent from some Dlp-expressing cells such as the mushroom body and the medulla neuropil glia (compare Figure 3D to Figures 1E and 1G, arrowheads).

Analysis of *sdc* null mutant larvae revealed that 50% of optic lobes had photoreceptor-projection abnormalities and/or lamina-plexus defects including gaps (29%) and gross disorganization (21%, n = 28) (Figures 3E–3G). Compared to *dlp* mutants, *sdc* mutants showed a low penetrance of the lamina-thickening (4%) and lamina-axon-crossover phenotypes (Figure S1C). Additionally, some *sdc* mutants had R7/R8-axon misrouting in the larval stage (Figure 3G, arrowhead). *sdc* mutant pupae showed crossover of R7 axons between medullary cartridges (100%, Figures 3H and 3I, insets) and defective axon pathfinding to the medulla (86%, Figure 3J, n = 21) but a low penetrance of R7/R8-termini disruption (~10%, see Figure S1D), a phenotype common in *dlp* mutants (80%–100%, Figure 2E, Figure S1B). As is the case for *dlp, sdc* mutants do not show defects in the specification of photoreceptors, glia, or lamina neurons (Figures S2–S4), confirming that the above phenotypes are not secondary to other overt patterning deficiencies. Overall, *dlp* and *sdc* mutants share similar axon-guidance phenotypes, but each has a largely distinct level of penetrance for a given defect.

Electrophysiological analysis revealed that *sdc* mutants have grossly abnormal ERGs, with defective photoreceptor depolarization and complete absence of on- and off-transients (Figure 4I). These ERG abnormalities—particularly the virtual loss of photoreceptor depolarization—are distinct from those found in *dlp* animals (Figure 2J). In addition, whereas *dlp* null mutants have a reduced and roughened eye, *sdc* mutants do not (Figures S2A–S2C). These findings are consistent

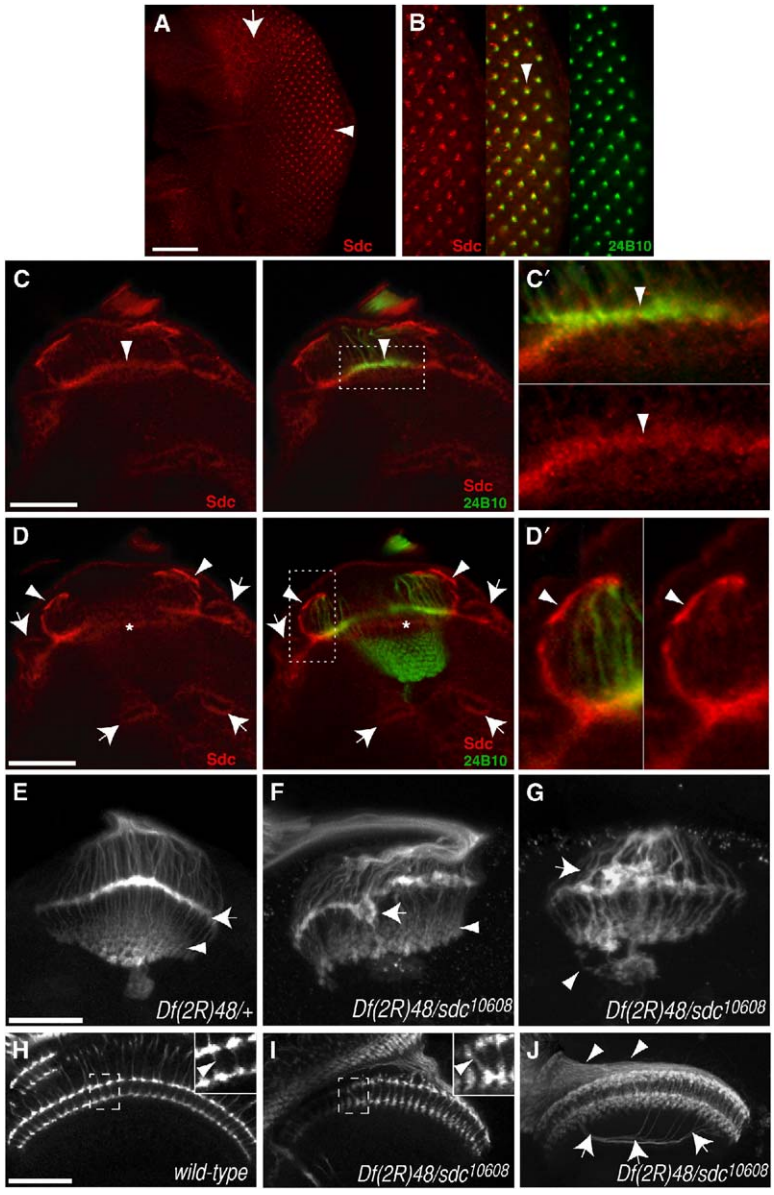

Figure 3. Sdc Expression and Function in the Developing Adult Visual System

(A–D) Anti-Sdc (red) and 24B10 (green) staining of wild-type third-instar eye-antennal disc and optic lobe (single optical sections). (C′) and (D′) show enlarged views of outlined regions. (A–B) Sdc colocalizes with differentiated photoreceptors (arrowheads) posterior to the morphogenetic furrow (arrow). (C, C′) Sdc is found throughout the length of the lamina plexus (arrowheads). (D, D′) Sdc expression is greatest on axons at the boundary of the lamina (arrowheads). These photoreceptors do not colocalize with 24B10, which only stains axons at more-mature stages of development (unlike GMR-driven expression of GFP as in Figure 1). Sdc is present at low levels on cells of the inner and outer proliferative centers (arrows), as well as just below the lamina plexus where the medulla glia are located (asterisks).

(E–G) Merged optical sections of 24B10 staining in third-instar larval brains. (E) *sdc* heterozygous control (lamina plexus [arrow], medulla [arrowhead]) is shown. (F, G) *sdc* mutants with disruption of lamina plexus (arrows) and with abnormal R7/R8 termini in the medulla (arrowheads) are shown.

(H–J) 24B10 staining of 40 hr pupal brains (single optical sections). (H) The wild-type optic lobe is shown. R7/R8 projections from each ommatidium (arrowhead on inset) remain in the same medulla cartridge. (I) *sdc* mutant pupae show crossover of R7 termini to neighboring cartridges (arrowhead on inset). (J) *sdc* mutant pupa with R7/R8-axon projections that deviate (arrows) from the proper route (arrowheads) to the medulla is shown. Scale bars represent 50 microns.

with distinct molecular functions for Dlp and Sdc during visual-system assembly.

Sdc and Dlp are both heparan sulfate-modified proteoglycans, and Dlp expression is capable of limited rescue of *sdc* axon-guidance abnormalities in the embryo [5]. To determine whether these two cell-surface molecules have overlapping functions in the visual system, we performed a series of rescue experiments. With or without a GAL4 driver, *dlp* mutant animals bearing a *UAS-dlp*$^{+}$ construct showed complete rescue of pupal axon-pathfinding defects (Figures 4B and 4C) and ERG abnormalities (data not shown), suggesting that low levels of Dlp expression are sufficient to provide the function necessary for normal axon guidance and visual-system assembly. Despite this, ubiquitous expression of Sdc was unable to rescue the axon-guidance abnormalities of *dlp* mutants (Figure 4D), demonstrating that Dlp and Sdc are not functionally interchangeable during photoreceptor axon guidance.

We also tested the ability of *UAS-dlp*$^{+}$ transgenes to rescue axon-guidance phenotypes of *sdc* mutant larvae and pupae. Pupal *sdc* mutant phenotypes, including misrouting of R7/R8 photoreceptors to the medulla and crossover of R7 to neighboring medulla cartridges, could be largely rescued with neuronal-directed expression of Sdc (Figures 4F and 4G). Conversely, neuron-specific expression of Sdc in *sdc* mutants was not sufficient to rescue photoreceptor projection defects to the larval lamina or the ERG abnormalities in adults (Figures 4J–4M and Figure 4I), suggesting that expression of Sdc in additional cell types is critical for complete restoration of axonal patterning and visual-system function. In contrast to the inability of Sdc expression to rescue *dlp* mutant phenotypes, neuron-

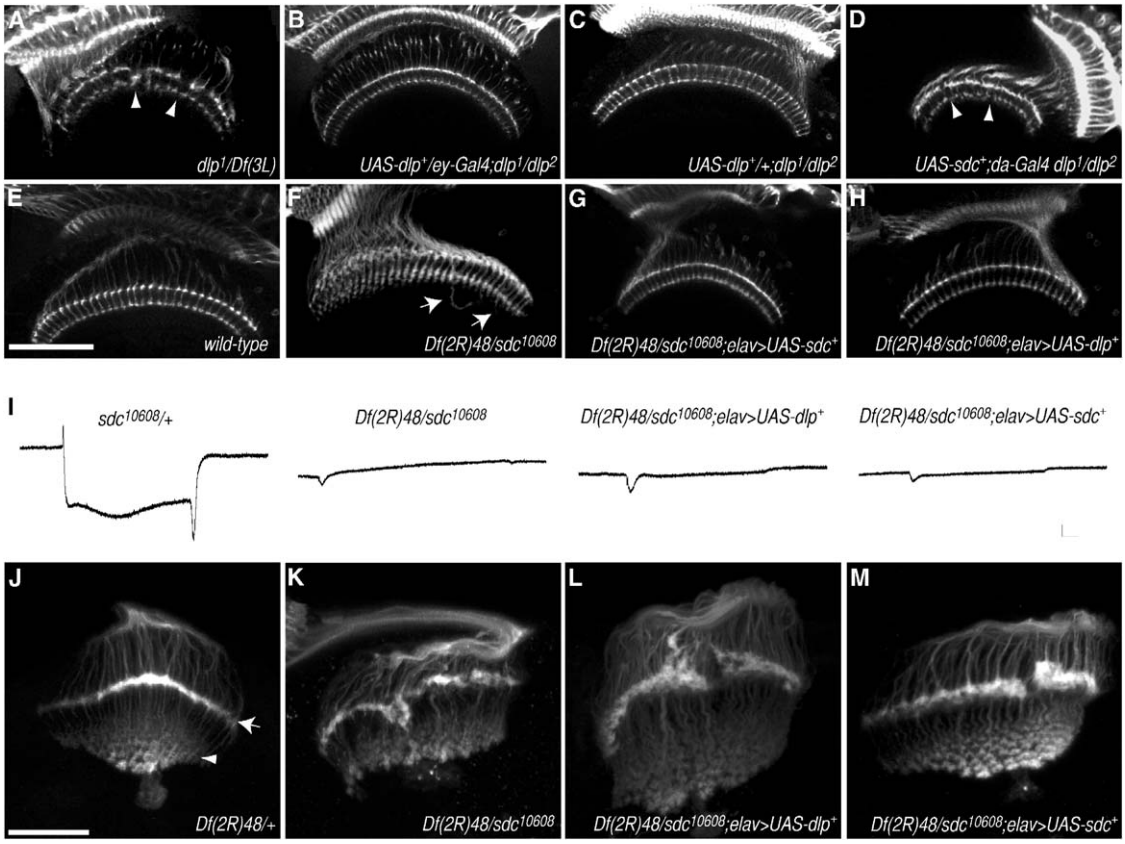

Figure 4. Transgene Rescue of *dlp* and *sdc* Mutant Phenotypes

(A–H) 24B10 staining of 40 hr pupal brains (single optical sections). (A) *dlp* mutants have defects in R7/R8 photoreceptor termination in the medulla (arrowheads). (B) Expression of *UAS-dlp*$^+$ under control of ey-GAL4 rescues the medulla patterning defects of *dlp* mutants. (C) *UAS-dlp*$^+$ transgene rescue of medulla patterning in the absence of a driver is shown. (D) *UAS-sdc*$^+$ is unable to rescue the medulla defects of *dlp* mutants (arrowheads), even under ubiquitous expression driven by da-GAL4. (E) The wild-type optic lobe is shown. (F) *sdc* mutants show misrouting of R7/R8 photoreceptor projections to the medulla (arrows). (G–H) Neuronal expression of *UAS-sdc*$^+$ or *UAS-dlp*$^+$ driven by elav-GAL4 rescues axon misrouting and crossover defects in *sdc* mutants.

(I) *sdc* mutant ERG profiles show severe defects in photoreceptor depolarization and in on- and off-transients. *UAS-sdc*$^+$ and *UAS-dlp*$^+$ both fail to rescue the ERG defects under neuron-specific expression. Scale = 3 mV, 200 ms.

(J–M) Projection of confocal sections (24B10 staining) in third-instar optic lobes. (J) A heterozygous control animal (lamina plexus [arrow], medulla [arrowhead]) is shown. (K) An *sdc* mutant with defects in R1–R6 termination, including large gaps and expansions in the lamina plexus, is shown. (L–M) *sdc* mutants are not rescued by neuronal expression of either *UAS-sdc*$^+$ or *UAS-dlp*$^+$.

Scale bars in (E) and (J) represent 50 microns.

specific expression of Dlp restored proper R7/R8 photoreceptor projection to the medulla of *sdc* mutant pupae (Figures 4E–4H). This rescue demonstrates that a structurally distinct HSPG can provide some of the functions normally served by Sdc.

In vertebrates, glypicans are expressed on axons and growth cones in the developing nervous system (reviewed in [8]). Whereas previous findings have established a function for glypicans in growth-factor signaling (reviewed in [18–20]), their role in axon guidance has not been reported. Consistent with the expression pattern of Dlp on axons and glial cells of the developing visual system, *dlp* mutants showed defects in photoreceptor projections to the lamina and medulla. Mosaic analysis demonstrated that Dlp is required on photoreceptors for some, but not all, aspects of axon guidance, serving functions in both peripheral and central components of the visual system. *dlp* was not required in the retina for normal electrophysiological responses to light, indicating that the synaptic-transmission defects in *dlp* mutant adults were due to loss of Dlp activity in the optic lobes.

Comparison of *sdc* and *dlp* mutants as well as transgene rescue experiments demonstrated that Sdc and Dlp have some overlapping functions in visual-system assembly but others that are unique. For example, photoreceptor misrouting to the medulla in *sdc* mutants can be rescued by neuron-specific expression of *dlp*$^+$, consistent with the capacity of *dlp*$^+$ to rescue midline-crossover defects in *sdc* mutant embryos [5]. In contrast to the ability of *dlp*$^+$ transgenes to rescue *sdc* mutants, *UAS-sdc*$^+$ constructs were unable to rescue any of the *dlp* mutant phenotypes, even under conditions where very modest levels of Dlp rescued completely. These findings show that Dlp functions cannot be readily provided by another unrelated HSPG, and they argue

that the conserved sequence elements of the Dlp core protein are critical for these unique functions.

Effects of HSPGs on axon pathfinding have been considered principally in the context of classical axon-guidance pathways, Slit-Robo signaling in particular. Although there is genetic evidence from mouse, *Drosophila*, and *C. elegans* that HSPGs affect Slit-Robo signaling, there are many other possibilities. HSPGs have been extensively characterized as molecules that affect both morphogen signaling and distributions (reviewed in [1]). Recent studies demonstrating that the classical morphogens Wnt, Hh, and BMP also play a bona fide role in axon guidance suggest the possibility that HSPGs govern axon guidance by affecting morphogen function or distributions during this process [21].

Supplemental Data

Detailed Supplemental Experimental Procedures and additional figures are available with this article online at http://www.current-biology.com/cgi/content/full/15/9/833/DC1/.

Acknowledgments

We thank Drs. S. Knox, C. Kirkpatrick, and H. Nakato for critical reading of the manuscript; the Bloomington Stock Center for fly stocks; the Developmental Studies Hybridoma Bank and Phil Beachy for antibodies; Tami Jauert for assistance with manuscript and figure preparation; and N. Khare for initial analysis of *dlp* mutants. This work was supported by the March of Dimes (contract grant number: 1-FY02-233) and by the National Institutes of Health (contract grant number: GM54832-09).

Received: September 9, 2004
Revised: March 7, 2005
Accepted: March 9, 2005
Published: May 10, 2005

References

1. Tabata, T., and Takei, Y. (2004). Morphogens, their identification and regulation. Development *131*, 703–712.
2. Inatani, M., Irie, F., Plump, A.S., Tessier-Lavigne, M., and Yamaguchi, Y. (2003). Mammalian brain morphogenesis and midline axon guidance require heparan sulfate. Science *302*, 1044–1046.
3. Bulow, H.E., and Hobert, O. (2004). Differential sulfations and epimerization define heparan sulfate specificity in nervous system development. Neuron *41*, 723–736.
4. Lee, J.S., von der Hardt, S., Rusch, M.A., Stringer, S.E., Stickney, H.L., Talbot, W.S., Geisler, R., Nusslein-Volhard, C., Selleck, S.B., Chien, C.B., et al. (2004). Axon sorting in the optic tract requires HSPG synthesis by ext2 (dackel) and extl3 (boxer). Neuron *44*, 947–960.
5. Johnson, K.G., Ghose, A., Epstein, E., Lincecum, J., O'Connor, M.B., and Van Vactor, D. (2004). Axonal heparan sulfate proteoglycans regulate the distribution and efficiency of the repellent slit during midline axon guidance. Curr. Biol. *14*, 499–504.
6. Steigemann, P., Molitor, A., Fellert, S., Jackle, H., and Vorbruggen, G. (2004). Heparan sulfate proteoglycan syndecan promotes axonal and myotube guidance by slit/robo signaling. Curr. Biol. *14*, 225–230.
7. Lander, A.D., Stipp, C.S., and Ivins, J.K. (1996). The glypican family of heparan sulfate proteoglycans: Major cell-surface proteoglycans of the developing nervous system. Perspect. Dev. Neurobiol. *3*, 347–358.
8. Yamaguchi, Y. (2001). Heparan sulfate proteoglycans in the nervous system: Their diverse roles in neurogenesis, axon guidance, and synaptogenesis. Semin. Cell Dev. Biol. *12*, 99–106.
9. Lum, L., Yao, S., Mozer, B., Rovescalli, A., Von Kessler, D., Nirenberg, M., and Beachy, P.A. (2003). Identification of Hedgehog pathway components by RNAi in Drosophila cultured cells. Science *299*, 2039–2045.
10. Kirkpatrick, C.A., Dimitroff, B.D., Rawson, J.M., and Selleck, S.B. (2004). Spatial Regulation of Wingless Morphogen Distribution and Signaling by Dally-like Protein. Dev. Cell *7*, 513–523.
11. Van Vactor, D., Jr., Krantz, D.E., Reinke, R., and Zipursky, S.L. (1988). Analysis of mutants in chaoptin, a photoreceptor cell-specific glycoprotein in Drosophila, reveals its role in cellular morphogenesis. Cell *52*, 281–290.
12. Heisenberg, M. (1971). Separation of receptor and lamina potentials in the electroretinogram of normal and mutant Drosophila. J. Exp. Biol. *55*, 85–100.
13. Poeck, B., Fischer, S., Gunning, D., Zipursky, S.L., and Salecker, I. (2001). Glial cells mediate target layer selection of retinal axons in the developing visual system of Drosophila. Neuron *29*, 99–113.
14. Huang, Z., and Kunes, S. (1996). Hedgehog, transmitted along retinal axons, triggers neurogenesis in the developing visual centers of the Drosophila brain. Cell *86*, 411–422.
15. Newsome, T.P., Asling, B., and Dickson, B.J. (2000). Analysis of Drosophila photoreceptor axon guidance in eye-specific mosaics. Development *127*, 851–860.
16. Lee, T., and Luo, L. (1999). Mosaic analysis with a repressible cell marker for studies of gene function in neuronal morphogenesis. Neuron *22*, 451–461.
17. Stowers, R.S., and Schwarz, T.L. (1999). A genetic method for generating Drosophila eyes composed exclusively of mitotic clones of a single genotype. Genetics *152*, 1631–1639.
18. Filmus, J., and Selleck, S.B. (2001). Glypicans: Proteoglycans with a surprise. J. Clin. Invest. *108*, 497–501.
19. Lin, X. (2004). Functions of heparan sulfate proteoglycans in cell signaling during development. Development *131*, 6009–6021.
20. Blair, S.S. (2005). Cell signaling: Wingless and glypicans together again. Curr. Biol. *15*, R92–R94.
21. Schnorrer, F., and Dickson, B.J. (2004). Axon guidance: Morphogens show the way. Curr. Biol. *14*, R19–R21.